ACTIVATED CARBON FROM PLANT-BIOMASS WASTE MATERIALS AS PROMISING ELECTRODES FOR SUPERCAPACITOR APPLICATIONS

A thesis presented to the Department of Material Science and Engineering
African University of Science and Technology, Abuja
In partial fulfillment of the requirements for the degree of

MASTER OF SCIENCE

By

OKAFOR CHIAMAKA CYNTHIA

Supervised by

Professor E. Ntsoenzok

African University of Science and Technology
www.aust.edu.ng
P.M.B 681, Garki, Abuja F.C.T
Nigeria

June 2016

APPROVAL PAGE

ACTIVATED CARBON FROM PLANT-BIOMASS WASTE MATERIALS AS PROMISING ELECTRODES FOR SUPERCAPACITOR APPLICATIONS.

By

Okafor Chiamaka Cynthia

A THESIS APPROVED BY THE MATERIALS SCIENCE AND ENGINEERING DEPARTMENT

RECOMMENDED: ----------

Supervisor, Prof E. Ntsoenzok

Dr M. G. Zebaze Kana

Dr D. Y. Momodu

Head, Department of Materials Science and Engineering

APPROVED: ----------

Chief Academic Officer

Date

ABSTRACT

This work is aimed at studying activated carbons as supercapacitor electrode materials derived from plant biomass waste materials. The activated carbon raw materials are sourced from coconut shell, pine cone and rice husk plant biomass. The chemical activation route is employed with KOH as an activating agent. The carbonization temperature used is 800 ^{o}C and the carbonization time is varied from 1 h to 5 h. Activated carbon of high surface area and porosity are achieved and their electrodes show a good electrochemical performance presenting them as applicable for supercapacitor electrode materials.

ACKNOWLEDGMENT

I acknowledge the favors of the Almighty God in my life especially through those who made this work a success. I want to acknowledge the African Capacity Building Foundation (ACBF) for sponsoring this program and the Pan African Materials Institute (PAMI) for funding this research work. Also, I sincerely appreciate the Materials Science and Engineering Lab in Kwara State University (KWASU) and Carbon Nanomaterials and Energy Research Group at the University of Pretoria for working with me. I also want to acknowledge the efforts of all my faculty, both visiting and resident, for their contribution towards making this program a success. My special acknowledgment goes out to the supervising team, Prof Esidor Ntsoenzok, Dr. M. G. Zebaze Kana, Dr. Damilola Y. Momodu, and all members of the energy research group at AUST for their contributions and encouragement. Finally, I appreciate all the input of my colleagues, friends and the AUST Community not forgetting the love and support showered to me by my family and friends. Thank you all so much!

DEDICATION

This work is dedicated to all Africans especially those whom through hard work strive to make the lives of others better. Also to the memory of the late Prof. O. O. Adewoye who inspired a lot in me in the very short while we interacted.

TABLE OF CONTENTS

LIST OF NOMENCLATURE

AAS	Aqueous Asymmetric Supercapacitors
AC	Activated Carbon
Ag/AgCl	Silver / Silver chloride
ASC	Asymmetric Supercapacitors
BET	Brunauer Emmett Teller
BJH	Barrett Joyner Halenda
CNT	Carbon Nanotubes
CP	ChronoPotentiometry
CV	Cyclic Voltammetry
CVD	Chemical Vapor Deposition
EC	Electrochemical Capacitors
ECP	Electrically Conducting Polymers
EDLC	Electric Double Layer Capacitor EDX
	Energy Dispersive Xray Spectroscopy
EIS	Electrochemical Impedance Spectroscopy
ES	Electrochemical Supercapacitors
ESR	Equivalent Series Resistance
FTIR	Fourier Transform Infrared Spectroscopy
GCD	Galvanostic Charge Discharge
KOH	Potassium Hydroxide
MWCNT	Multi-Walled Carbon Nanotubes
NMP	N-methyl-2-pyrrolydone
NPC	Nano-Porous Carbons
PAn	Polyaniline

PANI	Polyaniline
PEDOT	Poly-3-4-ethylenedioxythiophene
Ppy	Polypyrrole
PVDF	Polyvinylidene fluoride
Redox	Reduction-oxidation
SC	Supercapacitors
SEM	Scanning Electron Microscopy
SWCNT	Single-Walled Carbon Nanotubes
TEM	Transmission Electron Microscopy
XPS	X-ray Photoelectron Spectroscopy
XRD	X-ray Diffraction
Z’	Real Impedance
Z”	Imaginary Impedance
^{o}C	Degree Celsius

LIST OF FIGURES

CHAPTER ONE

INTRODUCTION

1.1 BACKGROUND

As the global economy constantly continues to rise, the global demand for power and energy sources are synonymously increasing. This raises the consumption of fossil fuels which produces two major related issues; depletion of fossil fuel reserves and environmental greenhouse emission problems which not only pose pollution problems but also climate change issues. These issues have been projected as one of the global urgent and important challenges to be tackled. There is, therefore, a need to develop alternative energy sources that are clean, sustainable, and meet up with the rising global demand. In view of this, a lot of renewable energy sources have been explored but they generally have a commonly associated issue; they are seasonal. Most renewable clean energy sources are highly dependent on the time of day and regional weather conditions. The need for the development of related energy conversion and energy storage devices, therefore, arises in order to take the harnessing of these renewable clean energy sources to their best efficiency. Energy conversion and storage devices showing the greatest potentials currently include; batteries, supercapacitors and fuel cells [1].

1.2 MOTIVATION AND PROBLEM STATEMENT

Supercapacitors are yet to reach their full potential even as energy storage problems persist. Supercapacitors are governed by the same fundamental equations as conventional capacitors, but utilizing higher surface area electrodes and thinner dielectrics to achieve greater capacitances seem to possess the quality for future energy solutions. Fossil-based carbon sources for application as activated carbon materials are limited and non- renewable; biomass-based sources are low-cost high-performance candidates.

1.3 SCOPE AND OBJECTIVE

This work is aimed at studying activated carbon which can serve as the negative electrode material of asymmetric supercapacitors. The activated carbon is sourced from biomass materials of pine cones, rice husks, and coconut shells. The electrochemical and surface area parameters of activated carbon are studied and a comparative study of the different materials is presented with suggested optimization techniques.

1.4 ORGANIZATION

This project work is organized into five chapters as follows;

- Chapter one, the introduction;
- Chapter two, the literature survey;
- Chapter three, the materials and methods;
- Chapter four, the results and discussion and
- Chapter five consists of a summary and concluding remarks.

CHAPTER TWO

LITERATURE SURVEY

2.1 ENERGY STORAGE

Electricity, a multi-sourced form of energy has one of its greatest challenges to be the ability to store and reuse stored energy fast and with convenience. The subject of energy storage still poses lots of associated issues which include; the density of storage and use as well as the lifecycle of devices. Batteries have been established to hold large amounts of energy after prolonged charging time while supercapacitors hold a little amount of power with very short charging time. Our growing global economy requires energy storage devices which will hold a large amount of energy in very short charging time and this can be achieved by a progressive development of supercapacitors to enable them to store large amounts of energy in their short charging time. Supercapacitors are a special kind of devices owing to their excellent cycling ability and high power density. They are at the forefront of tremendous ongoing research for new and hybrid energy technology developments aimed at arresting the pressing issues of rising global demands for clean sustainable energy. Supercapacitors have a limitation in the amount of energy they can store although they have good charging and discharging abilities, as such most supercapacitors presently in use are coupled to another energy source, usually batteries, to enable them to supply the needed energy over a given period of time. [1]

2.2 SUPERCAPACITORS (SCs)

Supercapacitors (often called an ultracapacitor) are electrochemical energy storage systems that store energy directly and physically as charge. Usually, capacitors can supply high specific powers, but the amount of energy stored is very low. Electrochemical capacitors (often called supercapacitors or ultracapacitors) can store reversibly a higher energy than regular capacitors and can be operated at substantially greater specific power than most batteries [2]. The early

concept of an electrochemical supercapacitor (ES) was based on the electric double-layer existing at the conductor-electrolyte interface. The electric double-layer theory was first proposed by Hermann von Helmholtz and further developed by Gouy, Chapman, Grahame, and Stern. The electric double-layer theory is the foundation of electrochemistry from which the electrochemical processes occurring at an electrostatic interface between a charged electrode material and an electrolyte are investigated [3]. Numerous electrochemical theories and technologies take root from this foundation, energy storage devices such as electrochemical supercapacitors, batteries, and fuel cells have been invented and established from these theories. Supercapacitors are governed by the same fundamental equations as conventional capacitors but utilize higher surface area electrodes and thinner dielectrics to achieve greater capacitances. Unlike batteries which depend on redox reaction mechanism for their operation, supercapacitors (SC) depend on the charge separation at the electrode/electrolyte interface for charge storage. When the SC is polarized, double layers are formed and oppositely charged ions are accumulated on the surface in a manner proportional to the applied voltage and energy is stored. The double layer formed consists of electric space charge from electrode where electrochemical reactions occur and ion space charge from electrode where chemical reactions occur. Electric Double Layer Capacitor (EDLC) are a nonfaradaic type of EC that do not allow any charge/mass transport across the electrode/electrolyte interface during charge storage such that the energy stored is purely electrostatic. The energy of the EC increases with increasing electrode parameter values such as the specific surface area, pore size distribution, electrical conductivity and wettability by the electrolyte. The maximum energy stored is given as;

$E = ½ CV^2$

Since the potential difference between conductors is given as;

V = Q/C, where Q is charge and is given as $Q = I \times t$

the work required to transfer a charge dQ is given as;

$$dU = VdQ = \frac{QdQ}{C}$$

such that energy of a charge, which is the work done in building up the charge from initial value, 0, to final value, Q, by adding dQ is;

$$\frac{1}{2}\frac{Q^2}{C} = \frac{1}{2}CV^2$$

 where $C = \frac{\varepsilon A}{d}$

for ε_o as dielectric constant, A as surface area, d as separation distance. Faraday discovered that C increases by a factor ε_o when an an insulator is put between the plates. ε is dependent on the nature of the insulating material and ε is dielectric constant having a value of 1 for vacuum. [4] As an electric field within capacitor reduces, the capacitance C increases i.e. voltage is lower for the same charge.

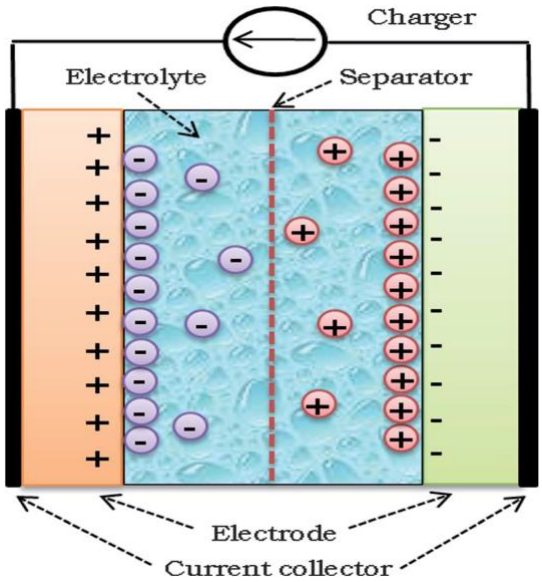

Figure 2.1: Schematic of simple electrochemical cell (Saswata Bose et al. 2012) [18]

Like an ordinary capacitor, a supercapacitor has two plates (also called electrodes) that are separated. The plates are made from metal coated with a porous substance such as powdery,

activated charcoal, which effectively gives them a bigger area for storing much more charge. In a supercapacitor, there is no dielectric as such. Instead, both plates are soaked in an electrolyte and separated by a very thin insulator (which might be made of carbon, paper, or plastic) [5]. This is why supercapacitors are often referred to as double-layer capacitors, also called electric double-layer capacitors or EDLCs. The capacitance of a capacitor increases as the area of the plates increases and as the distance between the plates decreases. In a nutshell, supercapacitors get their much bigger capacitance from a combination of plates with a bigger, effective surface area (because of their activated charcoal construction) and less distance between them (because of the very effective double layer).

The first supercapacitors were made in the late 1950s using activated charcoal as the plates. Since then, advances in material science have led to the development of much more effective plates made from materials such as carbon nanotubes, graphene, aerogel, and barium titanate [5]. The earliest ES patent was filed in 1957 however, not until the 1990s did ES technology begin to draw some attention, in the field of hybrid electric vehicles. It was found that the main function of an ES could be to boost the battery or fuel cell in a hybrid electric vehicle to provide the necessary power for acceleration, with an additional function being to recuperate brake energy. Further developments have led to the recognition that ES can play an important role in complementing batteries or fuel cells in their energy storage functions by providing backup power supplies to protect against power disruptions [6]. They can, therefore, promote constant power supply.

Supercapacitors have been widely used as the electrical equivalents of flywheels in machines as energy reservoirs that smooth out power supplies to electrical and electronic equipment. Supercapacitors can also be connected to batteries to regulate the power they supply as applied in wind turbines, where very large supercapacitors help to smooth out the intermittent power supplied by the wind. In electric and hybrid vehicles, supercapacitors are increasingly being used as temporary energy stores for regenerative braking where the energy of a stopping

vehicle which is normally wasted is briefly stored and then reused when it starts moving again. The capacity of ultracapacitors is largely determined by the electrode material and as a result, there has been dramatically increased research to improve the performance of electrode materials. While the energy density of ultracapacitors is very high compared to electrostatic and electrolytic capacitors, but it is still significantly lower than batteries and fuel cells [2] as seen in the figure below.

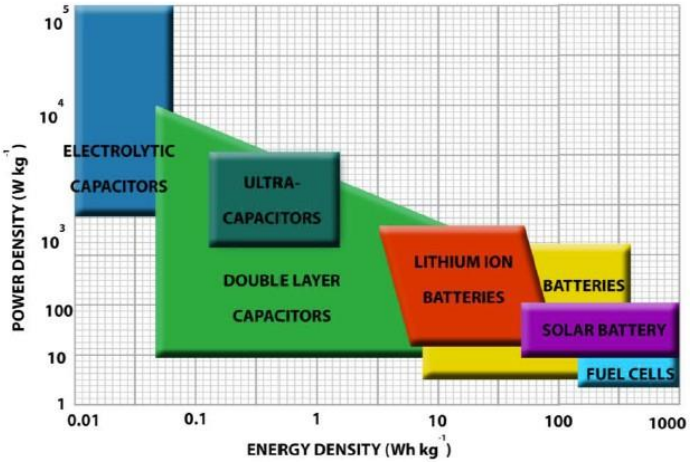

Figure 2.2: Ragone plot for common energy storage devices (D Y Momodu 2015) [19]

From Nernst equation, G = QΔE for battery and G = Q. ½ΔE for capacitors. This is because every additional element of charge added has to do electrical work against charge density accumulated on the plates, thereby increasing interelectrode potential difference. The pure capacitive behaviors appear as mirror images for positive and negative sweeps on voltammograms but different ranges of potentials are required for oxidation and reduction in batteries and as such their voltammograms are asymmetric. [7]

- To overcome this challenge, extensive work has been devoted to increasing the energy density of ESs, [1,2] in order to widen their application scope. Since the energy density (E) of ESs is proportional to the capacitance (C) and the square of the voltage (V), that is: $E = ½ CV^2$, increasing either or both of the capacitance and the cell voltage is an effective way to increase the energy density. This can be achieved through the development of electrode materials with high capacitance,

electrolytes (electrolyte salt + solvent) with wide potential windows, and integrated systems with a new and optimized structure, [8] thus leading to a continuous development of different supercapacitor types over the years. Supercapacitors based on their energy storage principle have been generally classified as;

- Electric double layer capacitors which operate in a fashion that creates for purely electrostatic charge double layer formation at the electrode electrolyte interface due to ion diffusion.
- Faradaic pseudocapacitors whose charge storage mechanism involves fast and reversible surface redox processes resulting from charge transfer through the electrode surfaces during electrosorption.
- Hybrid capacitors which involve a combination of both electric double layer and faradaic type process mechanisms. [9]

A basic classification of supercapacitors is given in the figure below;

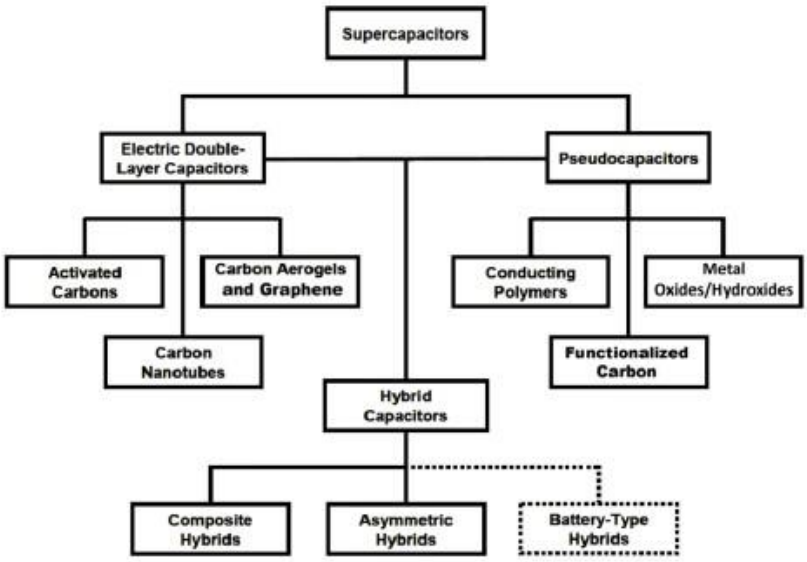

Figure 2.3: Classifications of Supercapacitors (M S. Halper, J C. Ellenbogen 2006)

2.3 ASSYMETRIC SUPERCAPACITORS (ASCs)

An asymmetric supercapacitor (ASC) is a type of hybrid supercapacitor based on two different electrode materials. One electrode is based on redox (Faradic) reactions with or without non-faradic reactions, and the other one is mostly based on electric double-layer (non-Faradic or electrostatic) absorption/desorption. Aqueous asymmetric supercapacitors (AASs) are promising hybrid energy storage devices as they have been shown to provide a wider operating voltage at higher energy density compared to symmetric capacitors. By combining a battery type electrode Faradaic cathode (transition metal oxide) material and a capacitor-type electrode anode material (usually an activated carbon). AASs make use of the different potential windows in the anode and cathode leading to an increased operational voltage of the aqueous electrolyte and significantly improving the energy density of devices. [9] Generally, most AASs make use of activated carbon (AC) as the negative electrode because of the anomalous pseudocapacitance mechanism at the surfaces of carbon-based electrodes when scanned at a negative potential in aqueous electrolytes. For the positive electrode, conductive polymers and various transition metal oxides are widely studied due to rapid and reversible electron exchange reactions at the electrode interface which contribute to the high energy and power densities of AASs. [1] AASs still face a challenge since all of their performance is at intermediate level.

2.4 ELECTRODE MATERIALS

To overcome the obstacle of low energy density, one of the most intensive approaches is the development of new materials for ES electrodes. Negative electrode materials for ASC are mostly carbonaceous materials usually porous carbon, carbon nanotubes, and graphene. Others include carbon aerogels, carbon nanocages and very rare oxides such as V_2O_5 and MoO_3. During the activation process of carbonaceous materials, modifications can be made by insertion of oxygen into carbon skeleton (oxidation) and plasma treatment can be used to introduce functional groups [10]. During the modification, oxidation for too long a timescale is

detrimental for carbon materials since it could reduce the surface area and electronic conductivity of the carbons, and impair their capacitive performance. The specific capacitance of ACs, is determined by both the ratio of edge/basal orientation and the nature of the functional group on the surface [10]. Considering the pore sizes, their influence on capacitance is closely related to electrolytes.

Carbon electrode materials generally have a higher surface area, lower cost, and more established fabrication techniques than other materials. Their action mechanism as negative electrodes is given as;

$$\text{Electrode} + C^{+} + e^{-} \rightarrow \text{Electrode/C (charging)}$$

$$\text{Electrode/C} \rightarrow \text{Electrode} + C^{+} + e^{-} \text{(discharging)}$$

Where C^{+} is cation and / is an interface with the electrode surface.

Porous carbons mainly include ACs and nanoporous carbons (NPCs). A variety of precursors are used for producing ACs such as charcoals, resins, petroleum coke, pitch and biomasses including waste paper. Since the action mechanism for capacitance is mainly due to absorption/desorption, the specific surface area, porosity and functional groups of ACs are important factors to achieve high energy density. The performance of porous carbons is dependent on a number of factors which include the nature of precursor material, type of activating agent, and conditions of activation and carbonization processes. In the case of NPCs, most are prepared by template methods so that the porosity and pore size can be tailored. When an external potential is applied to a porous carbon electrode, oppositely charged ions are absorbed on its pore surfaces and charge accumulation occurs at the electrode electrolyte interface, forming electric double-layers, thereby allowing electricity to be stored, and as such, they can be used for the non-Faradic side of ASCs.

Figure 2.4: Activated Carbon

CNTs, carbon nanotubes, have hollow tubes with diameters in the nanometer range and lengths usually at micro scale. Based on the number of tube walls, CNTs can be classified into single-walled carbon nanotubes (SWCNTs) and multi-walled carbon nanotubes (MWCNTs). The capacitive behavior of CNTs is similar to that of ACs but hetero-atoms doped CNTs exhibits pseudocapacitance through a faradic reaction in the framework or as functional groups on the surface. In both single and multi-walled CNTs, the electronic transport occurs over long tube ranges without electronic scattering and the network of large external small pores formed by the entanglement of the CNTs allows for fast solvated ion diffusion during charge and discharge processes [10]. This property makes them successful at carrying high densities of currents without energy dissipation. As a result, in most cases CNTs are often used in the form of composites but, the production costs of CNT-based supercapacitors is yet to meet acceptable performance.

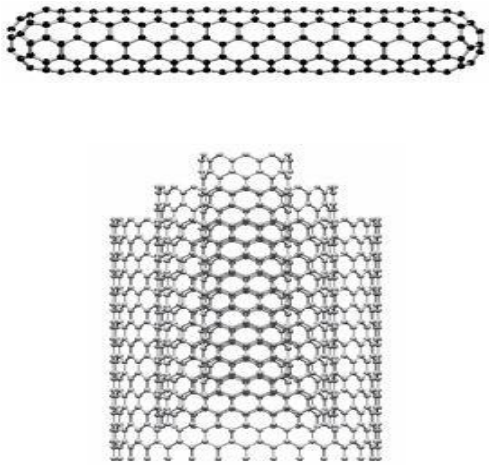

Figure 2.5: Carbon Nanotubes (Leo Daniel 2016) [20]

Graphene, a one-atom-thick 2D single layer of sp2-bonded carbon, possesses a unique two-dimensional structure and excellent mechanical, thermal and electronic properties and can be prepared by several kinds of methods. [10] The properties of graphene can be greatly affected by the number of layers and the degree of surface reduction or oxidation. Graphene can also be activated to achieve ultraporous graphene as the negative electrode for ASCs. However, aggregation and restacking are still a major hurdle that limits graphene-based nanocomposites from realizing their full performance, which causes inferior ionic accessibility and electrochemical performance. Graphene can also form composites with other kinds of carbon and electrochemically active materials such as polyaniline (PAn), and polypyrrole (PPy).

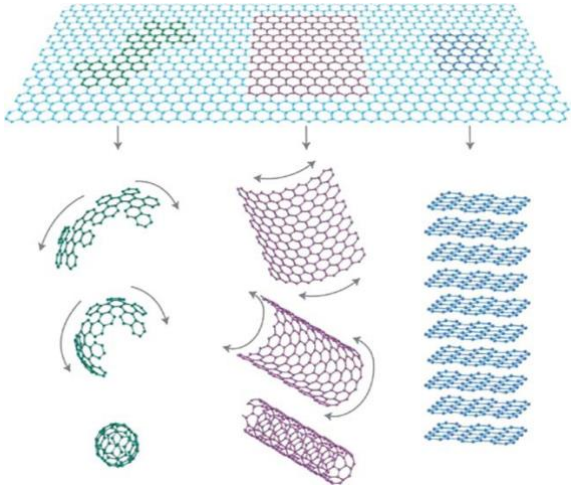

Figure 2.6: Graphene, mother of all graphitic carbon (L L Zhang et al. 2010) [21]

Positive electrode materials for ASCs include oxides, conducting polymers, some carbonaceous materials and intercalation compounds. The carbonaceous materials could be used in composites with one another or the oxides. The action mechanism of carbonaceous materials as positive electrodes is given as;

$$\text{Electrode} + A^- \rightarrow \text{Electrode}/A + e^- \quad \text{(charging)}$$

$$\text{Electrode}/A + e^- \rightarrow \text{Electrode} + A^- \text{ (discharging)}$$

Where A^- is anion and / is interface with electrode surface.

Transition metal Oxides are also used as electrode materials for supercapacitors owing to

their pseudocapacitance property. Most widely used metal oxide is RuO2, others include NiO, MoO3, and MnsO2 etc. These group of electrode materials possess high psuedocapacitive and high stability properties and also perform well in composites but suffer draw backs such as unavailability, high cost.

Conducting polymers have been used extensively as supercapacitor electrode materials. The most attractive include Polypyrrole (PPy), Polyaniline (PANI), and Poly-3,4-ethylenedioxythiophene (PEDOT) because of their quick redox reactions. The possible application of electronically conducting polymers, ECPs, in electrochemical capacitors is dictated by their significant capacitance values [6, 11, 12, 13]. Contrarily to activated carbons where only the surface is used for charge accumulation, in the case of ECPs, the total mass and volume is involved in charge storage. Extremely high capacitance values can be obtained with a thin ECP film electrodeposited on a conducting support like Pt and/or glassy carbon. The values reported for different ECPs, e.g. PANI can easily reach values of $1000Fg^{-1}$ when the electrochemical investigation is performed in a three electrode cell using a thin film that has a very limited use for a practical supercapacitor operating as a two-electrode system [13]. The main drawback of ECPs application as supercapacitor electrodes is connected with their poor stability during cycling. The ECP films, due to volumetric changes during the doping/dedoping process (insertion/deinsertion of counter ions), undergo swelling, shrinkage, cracks or breaking that in consequence gradually aggravates their conducting properties.

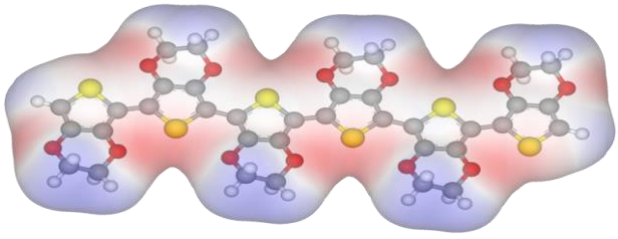

Figure 2.7: PEDOT Electronic conducting polymer (geoffhutchison.net)

2.5 ELECTROLYTES

Electrolytes have been identified as some of the most influential components in the performance of electrochemical supercapacitors (ESs), which include: electrical double-layer capacitors, pseudocapacitors and hybrid supercapacitors. These electrolytes contain ions for charge transport and storage and are generally classified as; organic, aqueous or ionic liquid electrolytes. Both energy and power densities are proportional to the square of operating voltage which can be determined by the decomposition voltage of the electrolyte. An ideal electrolyte should, therefore, have a wide voltage window, high conductivity, excellent electrochemical stability, small solvated ionic radius, high ionic concentration, low viscosity, high purity, environmentally friendly, low cost and readily available. [14]

Aqueous electrolytes are generally non-flammable, having low viscosity, low cost, and excellent safety. They are disadvantaged because they have low voltage window due to the thermodynamic decomposition of water at 1.229 V and low overpotential for hydrogen evolution reaction [14]. Notable aqueous electrolytes include; KOH, H_2SO_4, Na_2SO_4 and should be deaerated before the electrochemical measurements to get rid of dissolved oxygen.

Organic electrolytes offer high specific capacitance and maximum working voltage thus increasing to a great extent the energy density of supercapacitors while maintaining its power density and cyclic stability. They have drawbacks of high cost, flammability, toxicity, large solvated ions, high viscosity, high internal resistance, low conductivity and low power delivery. Organic electrolytes are prepared from organic salts such as Et_4NBF_4, $TEABF_4$, $(C_2H_5)_4PBF_4$ using organic solvents, typically acetonitrile and propylene carbonate to provide mobile ions. **Ionic liquids** which are room temperature molten salts with melting temperatures at or below room temperature and composed entirely of highly asymmetric combination of anion and cation have unique properties including low vapor pressure, high thermal and chemical stability, low flammability, a wide electrochemical voltage window, and higher conductivity compared to organic electrolyte. However, ILs have some disadvantages such as a

relatively high cost, high viscosities, and low ionic conductivity at room temperature. The commonly used ILs for the applications in supercapacitor are imidazolium, pyrrolidinium, tetrafluoroborate, trifluoromethanesulfonate, bis(trifluoromethanesulfonyl)imide, bis(fluorosulfonyl)imide, or hexafluorophosphate.

The aqueous electrolytes are preferred because they have inherent advantages over organic electrolytes. Some of which include; low cost, safety, ionic conductivity and smaller solvated ions.

2.6 PROCESSING METHODS FOR ACTIVATED CARBON

The electrode material is a key component in determining a supercapacitor's capacity. There are numerous processing methods and routes through which supercapacitor electrodes are achieved. Activated carbon on its own part has a number of ways in which it can be synthesized from its precursor material and these processing methods are aimed at optimizing its performance as electrode materials. Numerous tests can be carried out on a processed supercapacitor electrode but the most definitive test for a new electrode material is how it performs in a full-scale commercial supercapacitor [2]. However, owing to the fact that there are numerous samples to be tested at the laboratory stage, it is not usually convenient and practical to develop a full-scale supercapacitor for the testing and as such the electrode materials are tested without assembling them into a complete device.

There are two basic methods to prepare ACs: physical and chemical activation. The former involves gasification of the carbon produced from carbonization with an oxidizing gas such as air, CO_2 and water vapor at elevated temperatures. In the case of the latter, carbonization and activation are carried out by thermal decomposition of the precursor impregnated with a chemical activating agent, such as $ZnCl_2$, KOH, K_2CO_3, HNO_3 or H_3PO_4.

Hydrothermal treatment

This is pre-treatment done before activation of the raw material carbon. This step is required to enhance the whole process as it results in a more effective use of the activating agent thus

optimizing final properties of the activated carbon. This process proceeds under elevated pressure and temperature.

Activation

Activation is a process involving the partial oxidation of carbon based materials such that carbon residues blocking pores are removed by burning. The process is aimed at increasing surface area and porosity of the material which can be enhanced by further burn off and use of activation agents such as; KOH, NaOH, H_3PO_4, $ZnCl_2$. The carbon material formed has a well-developed and readily accessible pore structures with pores of controllable size. The activation of carbon could be chemical or physical.

Physical activation of carbon proceeds in the presence of carbon gasification reactants such as CO_2, air, and H_2O. It involves reactions between the carbon and oxidizing gas to create pores. Physical activation is considered environmentally friendly as it uses gaseous activating agents which do not produce waste water but has a poor yield, consumes much time and energy as well as poorly developed pore structures.

Chemical activation of carbon, on the other hand, involves the use of activating agents such as KOH and NaOH which function as dehydrating agents that prevent the formation of tar and hence promote the carbon yield during pyrolytic decomposition. Chemical activation generates good carbon yields but activating hydroxides are very corrosive.

The main advantages of chemical activation over physical activation are higher yield, lower temperature of activation, less activation time and generally higher development of porosity. It also preserves the shape of raw materials causing less surface damage and maintaining morphology [15]. The disadvantages include more expensive activating agents and also necessary additional washing stage required. The activation process is strongly affected by the carbon to activating agent ratio, C:KOH ratio, temperature and time. When using KOH as an activating agent, the total activation process is quite complicated and

proceeds via different pathways and by-products.

The following reactions can be considered:

$$4\ KOH + C \rightarrow K_2CO_3 + K_2O + 2\ H_2 \quad [16]$$

Recently, some processes including laser ablation, electrical arc, chemical vapor decomposition (CVD) and nanocasting, which do not include activation processes, can also be used to prepare ACs.

Carbonization

This is a pyrolysis (heating in the absence of oxygen) of carbonaceous materials which involves the complex processes of many reactions such dehydrogenation, condensation, isomerism, hydrogen transfer to achieve a carbon yield of the starting precursor material. Carbonization processes are usually carried out in a tubular furnace or in a microwave assisted process.

Evaluation of electrodes

Various characterization and measurement can be carried out on activated carbon for the purpose of supercapacitor electrodes. Such characterization techniques include;

Scanning Electron Microscopy (SEM), Transmission Electron Microscopy (TEM), which are used to study the structure and morphology of the AC samples. Energy Dispersive X-ray spectroscopy (EDX), to determine the chemical composition of the specimen. Gas adsorption analysis which is used for surface area measurement with the Brunauer Emmett Teller (BET), method and also for pore volume and size distribution which is obtained using the Barrett Joyner Halenda (BJT), method. XPS for elemental composition, Raman analysis for further chemical and structural analysis and FTIR to probe the surface chemistry of the sample and presence of functional groups. Electrochemical measurement electrode test can be carried out with two and three electrodes configurations. In the three-electrode assembly, measurements are achieved

using the electrochemical impedance spectroscopy (EIS) for ion transport mechanism, Galvanostatic charge-discharge, GCD, also known as chronopotentiometry (CP), for charge storage mechanism and cyclic voltammetry (CV), for thermodynamics of electrochemical reactions of the system.

2.7 PRIOR WORKS

Li Sun et al. [17] already showed that the large surface area porous graphene-like nano sheets (PGNs) synthesized by simultaneous activation-graphitization (SAG) sourced from renewable biomass waste coconut shell exhibited high specific capacitance ($268Fg^{-1}$) better than; activated carbon ($210Fg^{-1}$) from only activation and graphitic carbon ($117Fg^{-1}$) from only graphitization, with superior cycle stability and columbic efficiency after 5000 cycles in KOH. AbdulHakeem Bello et al. [22] also reported transformation of readily available pine cone biomass to porous carbon by KOH activation and carbonization, achieving a specific surface area of 1515 m^2g^{-1}, a high voltage window of 2.0 V, a gravimetric capacitance of 137 Fg^{-1}, energy density of 19 $Whkg^{-1}$ and excellent cyclability but observed low electrochemical performance resulting from pore texture. Oxygen doped KOH activated carbon sourced from three different biomasses were recently prepared by Wanru Feng et al. and in addition to an excellent cycling performance, a high surface area of $911.2m^2g^{-1}$ and high specific capacitance of $286.9Fg^{-1}$ at $0.5Ag^{-1}$ from waste dragon fruit skin [23]. Also, Xiaojun He et al. took a one step microwave assisted $ZnCl^2$ activation route of mesoporous carbon from rice husk biomass material and achieved $1737m^2g^{-1}$ surface area and $157Fg^{-1}$ specific capacitance at $0.05Ag^{-1}$ [24]. Dabin Wang et al similarly synthesized biomass derived activated carbon from corn cob by chemical activation to achieve a high specific capacitance of $401.6Fg^{-1}$ in 0.5M H_2SO_4 and $328.4Fg^{-1}$ in 6M KOH aqueous electrolyte at $0.5Ag^{-1}$[25].

CHAPTER THREE

MATERIALS AND METHODS

3.1 SAMPLE SYNTHESIS

Activated carbon was made out of raw materials which included; pine cones, rice husks, and coconut shells.

Coconut shell was manually crushed to tiny pieces and washed with water to get rid of dirt and with acetone to rid volatiles such as oils. The washed samples were then oven dried to get rid of the moisture. Likewise, pine cones were washed with distilled water and acetone and oven dried as well. The samples of pine cones, rice husks, and coconut shells were treated in a hydrothermal treatment process by adding a solution of distilled water and sulphuric acid to the biomass precursors. Subsequently, they were autoclaved for 6hrs followed by thorough washing with distilled water and oven drying at 80 ^{o}C. The activation process proceeded with a chemical activation method which was carried out with KOH activating agent. A solution of 2 M KOH was prepared and used to impregnate individual biomass sample for 24 hr in a KOH to sample weight ratio of 1:1. Activated samples were dried at 80^{o}C for 1hr afterward, they were then transferred into crucibles for carbonization at an optimized temperature of 800 ^{o}C in a tubular furnace for varying carbonization holding time of 1 hr, 2 hr, 3 hr, 4 hr and 5 hr. The carbonization was carried out under argon flow of 10cm^{3}/min and the temperature was ramped from room temperature at 20 ^{o}Cmin^{-1} up to 800 ^{o}C and held at a varying time for the same temperature. Also, control samples for each biomass source were activated and carbonized with a holding time of 1hr at 800 ^{o}C without previously undergoing hydrothermal treatment. The carbonized samples were cooled to room temperature after carbonization in a furnace under argon flow to avoid oxidization of samples at high temperature and proper arrangement of atoms as in an anneal cooling process.

All samples were activated in a C:KOH ratio of 1:1 but were carbonized at various holding times. This will enable the study of carbonization time effects on the various biomass sourced activated carbon samples for supercapacitors electrodes. After the carbonization process, each sample was soaked in 0.1 M HCL solution for 24 hr to dissolve all the unreacted KOH that may be left in the activated sample and then washed repeatedly with deionized water to bring them to neutral pH followed by drying at 80 ^{o}C in an oven.

Samples were required for the proximate analysis which required the percentage moisture content, ash content and volatile matter content for the determination of the fixed carbon content (FC), of the respective biomass sourced carbonaceous material.

FC = 100 – (%MC + %AC + %VM)

In order to determine the moisture content (MC) of the samples, 1 g of the sample powder was heated in an oven at 105 ^{o}C for 1 hr. The weights of sample powder were taken before and after the heating process in the oven and the percentage moisture content can be calculated thus;

$$\%MC = \frac{weight\ loss}{initial\ weight\ of\ sample} \times 100$$

also, to determine the ash content (AC) of the samples, 1 g of sample powder was allowed complete combustion in a furnace at 750 ^{o}C and the weight of samples were taken before and after the combustion process. The percentage ash content can be calculated thus;

$$\%AC = \frac{weight\ of\ residue}{initial\ weight\ of\ sample} \times 100$$

likewise, the volatile matter content, VM, was determined by taking weights of samples before and after a heating process of 1 g of sample powder in a furnace at 950 ^{o}C for 7 minutes in absence of air. Percentage volatile matter content can be calculated thus;

$$\%VM = \frac{weight\ loss}{initial\ weight\ of\ sample} \times 100$$

3.2 MATERIALS CHARACTERIZATION

Scanning electron microscopy

The scanning electron microscope (SEM) was used to test for sample surface morphology of samples held in the sample holder of the instrument. This was achieved by scanning the samples with a high-energy beam of electrons in a scan pattern such that the electrons interact with the atoms of the samples. This produced signals that contained useful information about the sample. In this work, the SEM images were obtained on a Zeiss Ultra Plus 55 field emission scanning electron microscope (FE-SEM) operated at an accelerating voltage of 2.0 kV.

Gas adsorption

The gas adsorption test was carried out by allowing nitrogen gas, N_2, to be adsorped and desorped by the samples. Nitrogen adsorption–desorption isotherms were measured at 196 ^oC using a Micromeritics ASAP 2020. All the samples were degassed at 180^oC for more than 12 hrs. under vacuum conditions. The surface area was calculated by the Brunauer Emmett Teller (BET) method from the adsorption branch in the relative pressure range (P/P_0) of 0.01 – 0.2.

Electrode fabrication

The fabrication of the electrodes are as follows; 85 wt% of the synthesized AC was mixed with a 10 % polyvinylidenefloride (PVDF) binder and 5 % carbon black to improve the conductivity. Nickel foam is a porous material serving as the electrical collector on which the activated carbon was coated. The mass of electrode material deposited on the nickel foam was calculated by subtracting the initial mass of the nickel foam from the final mass of the coated nickel foam after drying.

Electrochemical measurement

All electrochemical measurements were carried out using a Biologic VMP-300 potentiostat. It involved measurements such as cyclic voltammetry (CV), chronopotentiometry (CP) and electrochemical impedance spectroscopy (EIS) which were performed in the frequency range

of 100 kHz – 1 MHz. The as-prepared ACs served as the working electrode, glassy carbon plate as the counter electrode and Ag/AgCl (3 M KCl) as the reference electrode in 6 M KOH electrolyte.

CHAPTER FOUR

RESULTS AND DISCUSSION

4.1 PROXIMATE ANALYSIS

This was used to determine the moisture content, ash content, volatile matter content and fixed carbon percentages of individual biomass sourced sample. The moisture content (%MC) can be calculated from measured values of sample powder and is calculated as;

Before and after weight values of sample powder are 1 g and 0.935 g respectively, therefore,

$\%MC = \frac{0.065}{1} \times 100 = 6.5wt\%$ for coconut shell biomass

Before and after weight values of sample powder are 1 g and 0.744 g respectively, therefore,

$\%MC = \frac{0.256}{1} \times 100 = 25.6wt\%$ for pine cone biomass

Before and after weight values of sample powder are 1 g and 0.918 g respectively, therefore,

$\%MC = \frac{0.082}{1} \times 100 = 8.2wt\%$ for rice husk biomass

The ash content (%AC) can be calculated from measured values of sample powder and is calculated as;

Before and after weight values of sample powder are 1 g and 0.253 g respectively, therefore,

$\% AC = \frac{0.253}{1} \times 100 = 25.3\ wt\ \%$ for coconut shell biomass

Before and after weight values of sample powder are 1 g and 0.061 g respectively, therefore,

$\% AC = \frac{0.061}{1} \times 100 = 6.1\ wt\ \%$ for pine cone biomass

Before and after weight values of sample powder are 1 g and 0.324 g respectively, therefore,

$\% AC = \frac{0.324}{1} \times 100 = 32.4\ wt\ \%$ for rice husk biomass

The volatile matter (%VM) content can be calculated from measured values of sample powder

and is calculated as;

Before and after weight values of sample powder are 1 g and 0.496 g respectively, therefore,

$\%VM = \frac{0.504}{1} \times 100 = 50.4\ wt\%$ for coconut shell biomass

Before and after weight values of sample powder are 1 g and 0.402 g respectively, therefore,

$\%VM = \frac{0.598}{1} \times 100 = 59.8\ wt\%$ for pine cone biomass

Before and after weight values of sample powder are 1 g and 0.530 g respectively, therefore,

$\%VM = \frac{0.470}{1} \times 100 = 47.0\ wt\%$ for rice husk biomass

4.2 YIELD

The activated carbon yield was also determined from the final weight of individual biomass sources before and after carbonization of the respective samples at a 5 hr holding time in the tubular furnace. The percent yield was determined from the relation:

$$\%Yield = \frac{w_i}{w_a} \times 100$$

where w_i and w_a were the initial weight of activated carbon before carbonization and weight of activated carbon after carbonization respectively.

Weight of activated carbon samples before carbonization were 9.605 g for pine cone biomass, 0.862 g for rice husk biomass and 9.701 g for coconut shell biomass while the weights after carbonization were 4.138 g, 0.410 g and 5.080 g respectively. Their percentage yields are therefore given as;

$\%Yield = \frac{5.080}{9.701} \times 100 = 52.37\ wt\%$ for coconut shell biomass

$\%Yield = \frac{4.138}{9.605} \times 100 = 43.08\ wt\%$ for pine cone biomass

$\%Yield = \frac{0.41}{0.862} \times 100 = 47.56\ wt\%$ for rice husk biomass

Table 4.1: Yield and Proximate analysis summary

Biomass source	%MC (Moisture content)	%AC (Ash content)	%VM (Volatile matter content)	%FC (Fixed carbon content)	%Yield
Coconut shell	6.5	25.3	50.4	17.8	52.37
Pine cone	25.6	6.1	59.8	8.5	43.08
Rice husk	8.2	32.4	47.0	12.4	47.56

The different biomass sourced activated carbons provided various fixed carbon content depending on the moisture content, ash content and volatile matter content present in the individual carbon source. The coconut shell for instance, had a fixed carbon content of about

17.8 wt% which when compared to the work of Mohd Iqbaldin et al. [1] and S. Dinesh [2] is reasonable for sourcing activated carbon.

The coconut shell based biomass activated carbon showed the highest yield and greatest fixed carbon content as seen on the table above and this was closely followed by the rice husk biomass. Therefore, the coconut shell biomass would produce the most quantity of activated carbon after the pyrolysis. This can simply mean that for a given mass of activated carbon, less of the coconut shell biomass is needed as compared to rice husks and pine cones and if they have the same cost per weight, it will also be the most economical choice all things being equal.

4.3 SCANNING ELECTRON MICROSCOPY

The microstructure and morphology of the various biomass derived carbon examined by field- emission scanning electron microscopy (FESEM) and the coconut shell control (without autoclaving) samples and 1hr carbonization samples are presented in **Fig. 4.1**. The low (**Fig. 4.1** (a)) and high (**Fig. 4.2** (b)) micrographs show that the

control samples possess porous carbon structure while the low (**Fig. 4.1** (c)) and high (**Fig. 4.1** (d)) micrographs show AC consisting of uneven densely packed porous carbon structures with underlying disintegration which seem to possess better porous structures than those of the control samples.

The images of **Fig. 4.2** show micrographs of samples carbonized for different times of 1hr (**Fig.4.2**(a)), 2hrs (**Fig.4.2**(b)) and 3hrs (**Fig.4.2**(c)). The number of porous sites on the sample surface was observed to increase with increasing carbonization time.

The micrographs of activated carbon derived from various biomass sources are shown in **Fig.4.3** where (**Fig.4.3**(a)) is AC from coconut shell, (**Fig.4.3**(b)) is AC from the pine cone and (**Fig.4.3**(c)) is AC from the rice husk.

In conclusion, an appreciable porosity is observed from the AC samples but it is still yet difficult to tell the surface area and pore size distribution from these images.

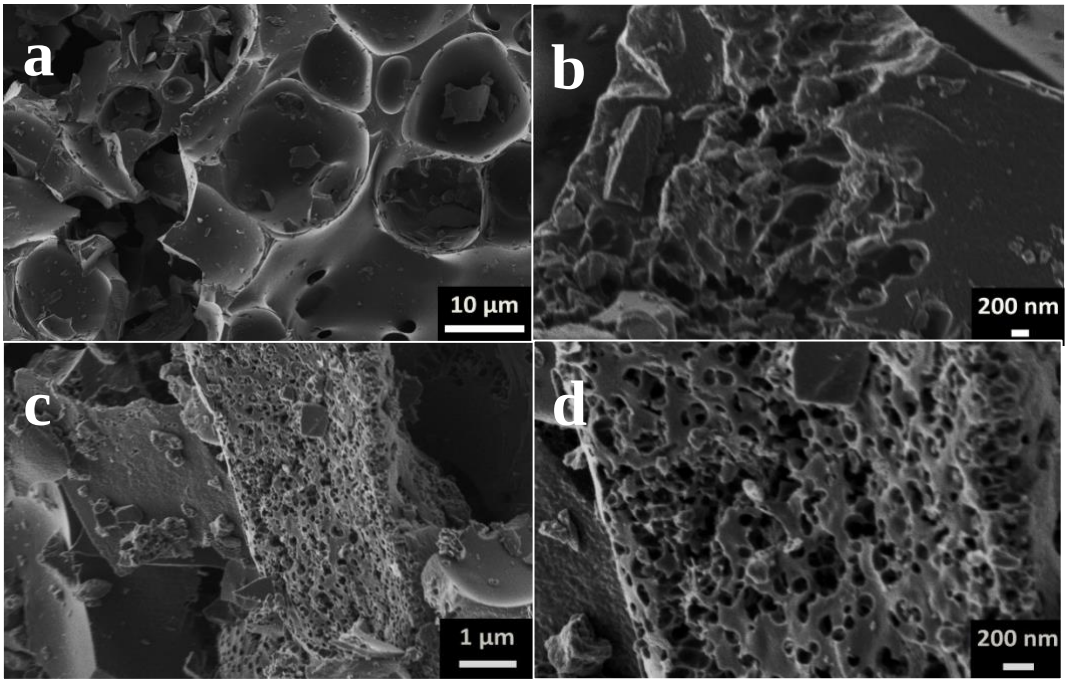

Figure 4.1: SEM images of control sample and 1 h carbonized samples from coconut shell at different magnifications

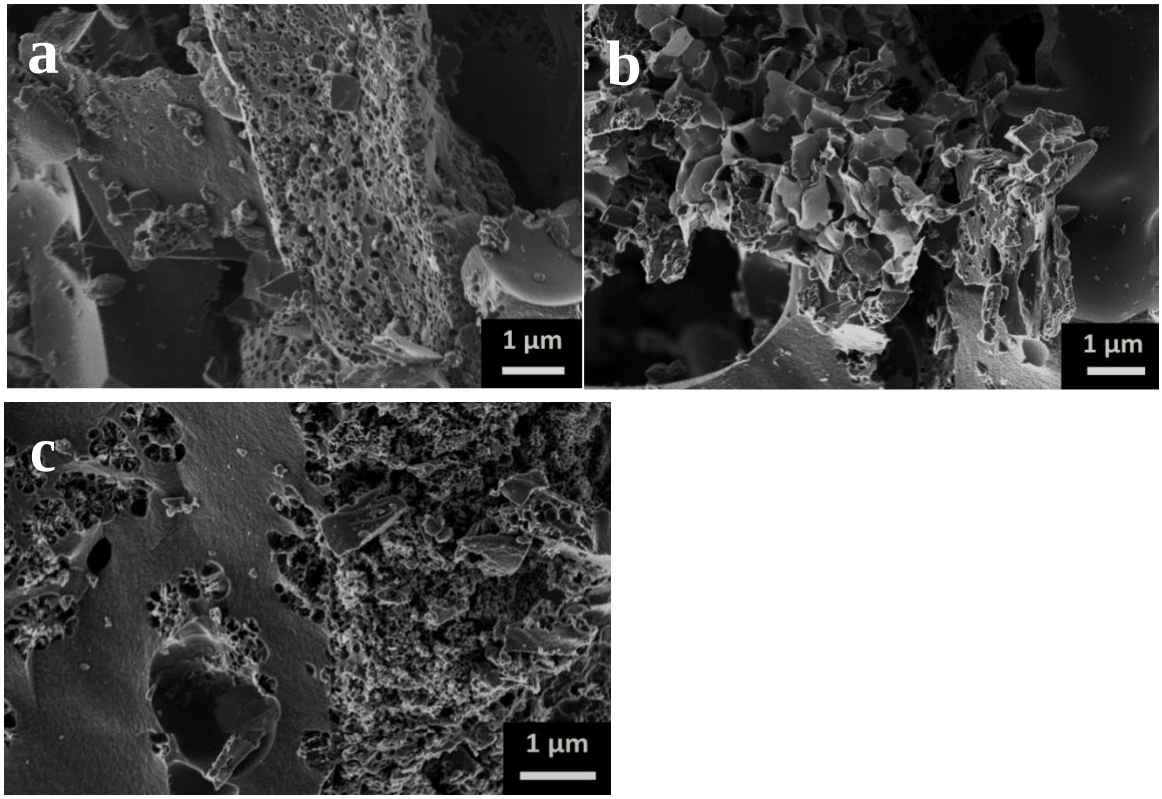

Figure 4.2: SEM images of 1 h, 2 h and 3 h carbonized samples from coconut shell

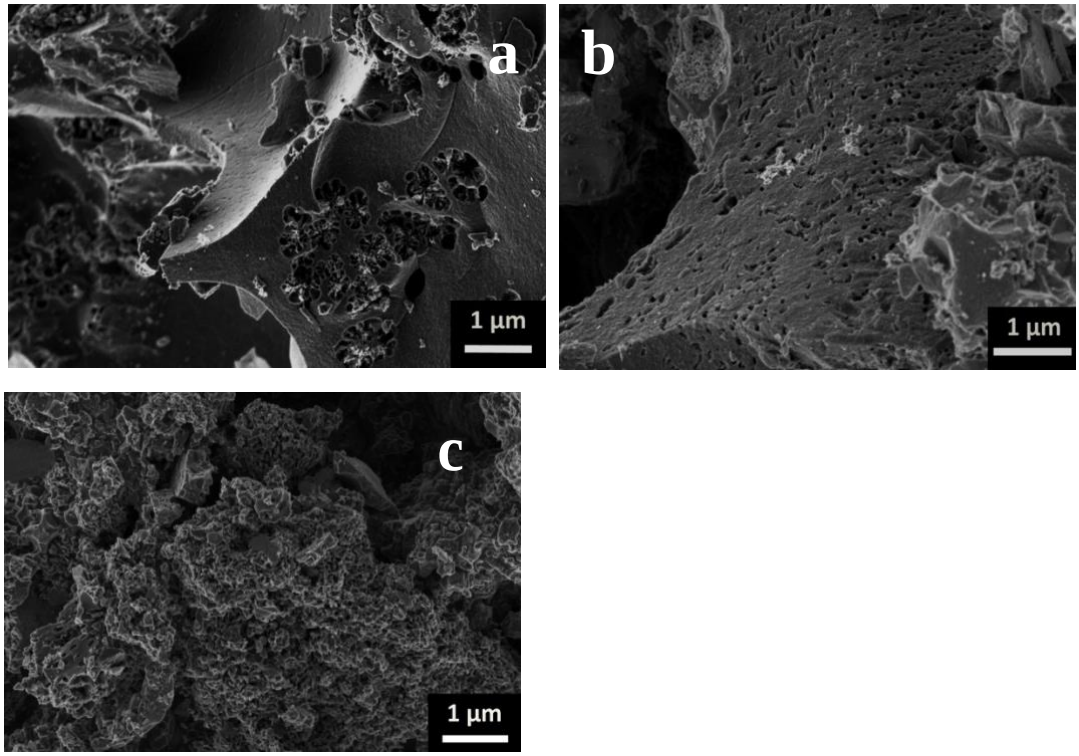

Figure 4.3: SEM image of 3 h carbonized sample from coconut shell, pine cone, and rice husk

4.4 ENERGY DISPERSIVE X-RAY ANALYSIS

Energy dispersive X-ray analysis was carried out on samples and **Fig. 4.4** shows the dispersive patterns of AC from coconut shell (**Fig.4.4**(a)), pine cone (**Fig.4.4**(b)) and rice husk (**Fig.4.4**(c)) all at 3 hr carbonization times as well as that of the control sample from the coconut shell (**Fig.4.4**(d)). It can be observed that all samples had high carbon concentration with other trace elements present which depended on the type of material and traces of activating agent left within samples. The variation in the composition of the ACs is dependent on their biomass sources and the highest degree of purity was observed for coconut shell derived AC.

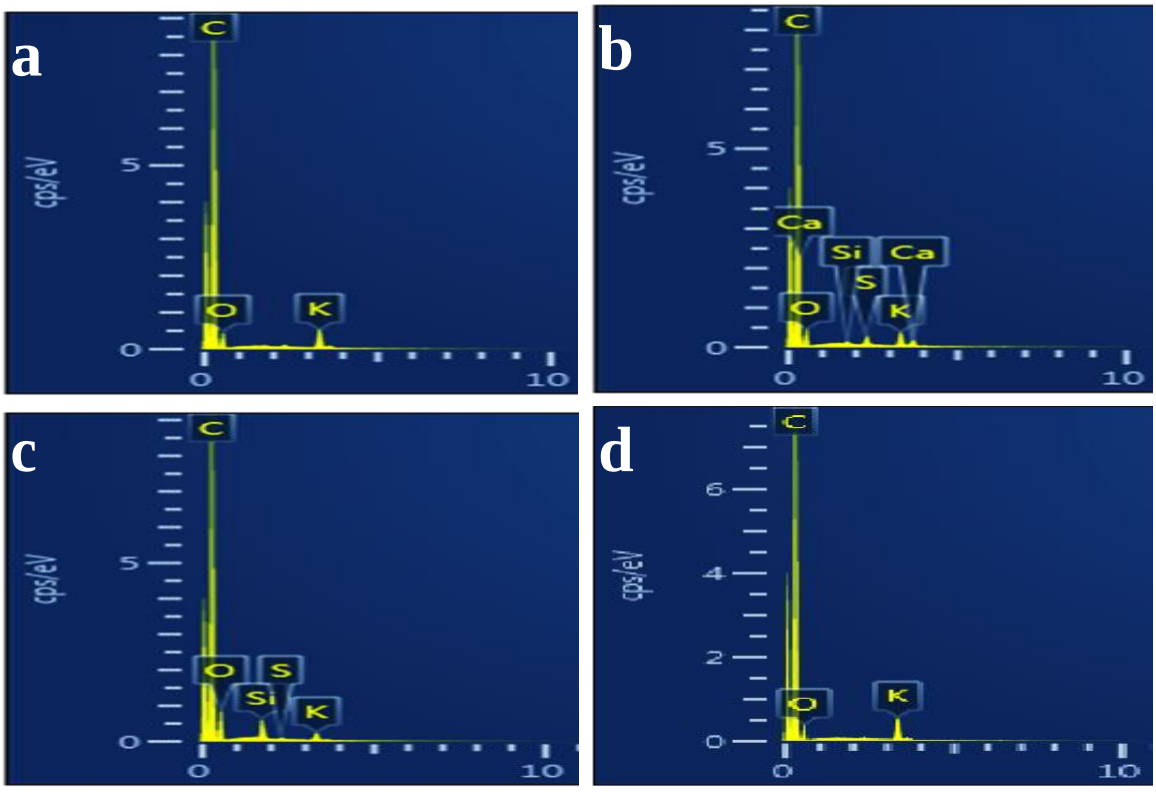

Figure 4.4: EDX Spectrum for AC samples from different biomass sources

4.5 GAS ADSORPTION MEASUREMENTS

The pore texture of the ACs was analyzed by N_2 adsorption/desorption measurements. **Fig. 4.5**(a) shows that the 1 hr carbonized sample and control sample ACs from pine cone biomass exhibits a type-II behavior with a H4-type hysteresis, suggesting a complex material containing both micropores and mesopores which according to IUPAC classification is

<2 nm for micropores and 2 - 50 nm for mesopores [3]. It is these pores that give rise to high surface areas as well as contribute to the measured capacitance. The Brunauer Emmett Teller (BET) specific surface areas (SSA) are 584.2 m^2g^{-1} and 456.7 m^2g^{-1} for the 1hr carbonized sample and control sample (without autoclaving) respectively. This is evident in the **Fig 4.5**(a) where the hysteresis loop for the autoclaved sample is really small compared to the control sample. The pore size distributions are shown in **Fig. 4.5**(b) and were calculated using the Barrett–Joyner–Halenda (BJH) analysis from the desorption branch and the pore size in the material is mainly distributed within 2 – 60 nm range with a mean value of about 6 nm. The higher surface area and narrower pore size distribution could be beneficial in charge storage as it provides high adsorbate accessibility and provides wider transport channels to micropores. The ACs possess a 3D porous structure as seen in the gas sorption analysis. Taking into account this combination of porosity, high surface area as shown in the isotherms and the microstructure in **Fig. 4.3**, the AC is expected to benefit charge storage through easy transport and mobility of the ion through the mesoporous pathways to the electrochemical active sites which are fundamental for efficient electrochemical performance.

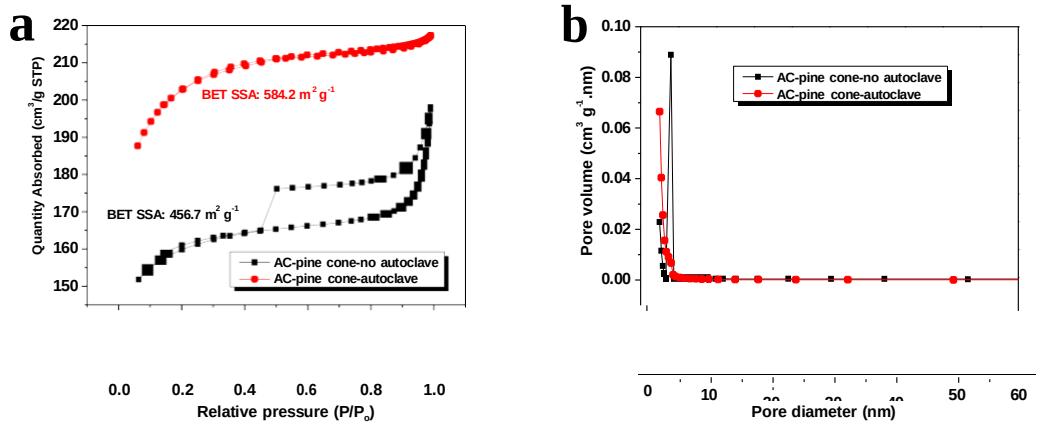

Figure 4.5: Gas adsorption measurement technique for pine cone samples

4.6 ELECTROCHEMICAL MEASUREMENTS

Cyclic voltammetry

Cyclic voltammetry (CV) is a well-known electrochemical technique for evaluating the

operating cell voltage and performance of ECs, and the results obtained are presented in **Fig4.6** The figure shows the CV of the various biomass derived activated carbon symmetric cell at a scan rate of 10 mVs^{-1} in 6 M KOH electrolyte solution, revealing distinctive symmetric rectangular shape typical for electrical double-layer charging behavior. More rectangular CV observed in **Fig. 4.6** (c) for the rice husk AC reveals a better and rapid charge propagation when compared to **Fig. 4.6** (a) and (b) for the coconut shell and pine cone respectively with distorted quasi-rectangular shapes. Thus, it presents the rice husk biomass sourced AC as possessing pure capacitive behavior since it is somewhat symmetrical [3]. **Fig. 4.6** (d) compares the CV for an autoclaved and un-autoclaved coconut shell at a scan rate of 10 mVs^{-1}. The behavior of both samples as seen in **Fig 4.6** (d) is approximately the same. Also, from the figure, it is observed that the AC electrodes from all three biomass sources are stable within the chosen potential window with predominantly EDLCs behavior.

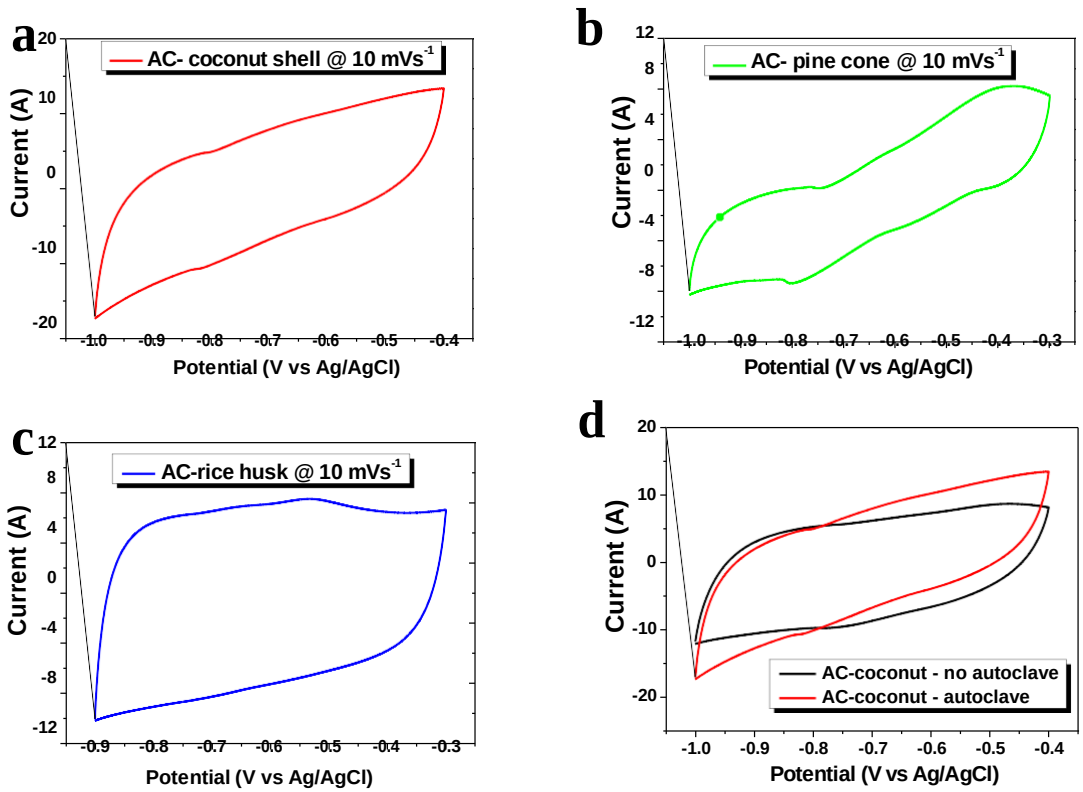

Figure 4.6: Cyclic voltammetry for activated carbons (ACs)

Galvanostatic Charge-Discharge

The constant current galvanostic charge discharge (CGCD) curves of symmetric cells are presented in **Figure 4.7** (a-c) for the three different biomass sources. The CGCD are triangular and proportional to each other emphasizing the electric double layer behavior observed in the CV curves of **Figure 4.6**. Also, the CGCD of the autoclaved and un-autoclaved coconut shell samples at a current density of 1 Ag^{-1} were compared in **Fig. 4.7** (d), showing that the autoclaved sample with longer discharge time exhibits the highest specific capacitance. The specific capacitance of all the electrodes were evaluated at a current density of 1 $Ag^{-1.}$ The specific capacitance of the electrodes was calculated based on the equation below;

$$C_s = \frac{i \times t}{m \times \Delta V}$$

where Cs is the specific capacitance (F/g), I is the discharge current (A), t is the discharge time (s), m is the mass (g) of active material and ∇V is the potential range of discharge (V). A maximum specific capacitance of 300 F/g was obtained for a 3 hr carbonized sample of coconut shell, 250.71 F/g for a 2 hr carbonized sample of pine cones and 161.17 F/g for a 2 hr carbonized rice husk sample which provided the best symmetry for the charge discharge measurement. Other specific capacitance values are presented in **Table 4.2**.

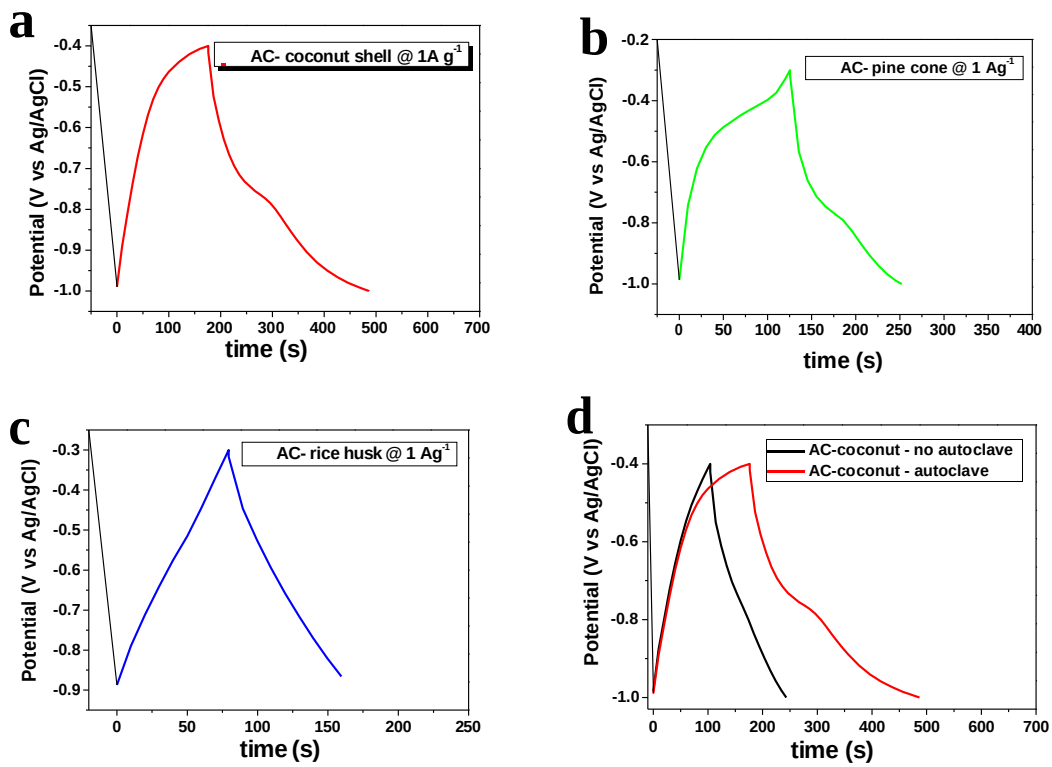

Figure 4.7: Constant current galvanostic charge discharge for ACs

Electrochemical Impedance Spectroscopy

In order to investigate the electrode/electrolyte interface behavior in detail, electrochemical impedance spectroscopy (EIS) measurements were employed at open circuit potentials. **Fig 4.8** shows the Nyquist plots of the ACs from different biomass sources as well as that of the control sample to further evaluate their electrochemical behavior at a frequency range of 10 mHz to 100 kHz. The figure shows the equivalent series resistance (ESR) which is the combined resistance of electrolyte, intrinsic resistance of substrate and contact resistance at the active material/current collector. The ESR value is obtained at the intercept of Z' axis (real part of the impedance) and the impedance curves are slightly tilted vertical lines indicating diffusion and charge transfer resistance of the electrodes. The slightly tilted vertical lines of the different biomass sourced electrode materials indicate a deviation from pure capacitive behavior where the imaginary impedance remains constant as the real impedance increases. The plot of the rice

husk derived sample which is the closest to vertical suggests a low diffusion resistance of ions within the structure of the material and thus implies it has the least parallel leakage reaction [4]. The lowest impedance value is for the rice husk plot and is read off at 0.66 Ω and other values are tabulated in **Table 4.2** shown below.

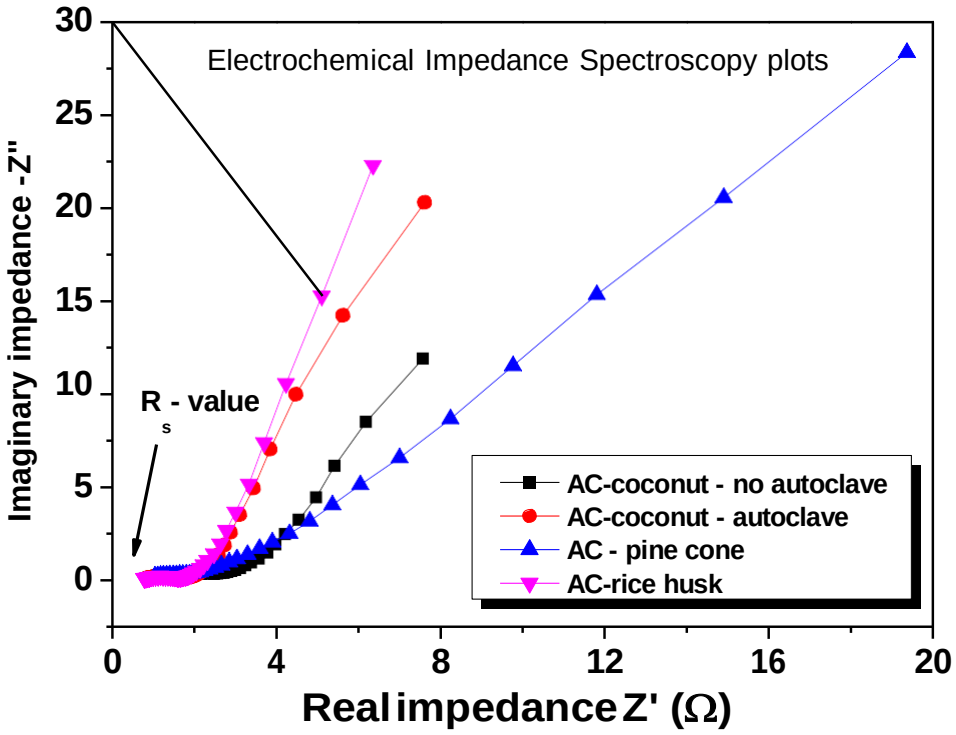

Figure 4.8: Nyquist Impedance plots of various AC samples

A summary of the electrochemical measurements carried out are presented in the table below displaying values of specific capacitance of selected samples and resistance of their various electrodes.

Table 4.2: Table of Electrochemical measurement summary

Sample electrode (AC-M-N)	**Specific capacitance (Cs in F/g) @ 1 A/g**	**Resistance of electrodes (Rs inΩ)**
AC-CO-0	**231.67**	**0.89**
AC-CO-1	115.00	0.81
AC-CO-2	191.67	0.79
AC-CO-3	300.00	0.88
AC-PC-0	**217.14**	**0.79**
AC-PC-1	214.29	0.92
AC-PC-2	205.71	0.81
AC-PC-3	181.43	0.81
AC-RH-0	**166.70**	**1.06**
AC-RH-1	125.00	0.66
AC-RH-2	161.17	0.80
AC-RH-3	148.33	0.80

Where for AC-M-N, AC is activated carbon, M is the biomass source of activated carbon with CO representing coconut shell, PC representing pine cone and RH representing rice husk, N is the carbonization time with exception of '0' which represents the control sample of the individual biomass source.

To summarize, the results presented so far have presented the waste plant-biomass materials under study as competitive materials for supercapacitor electrodes. This is evident **Table 4.3** below;

Table 4.3: Summary of supercapacitor study

Author	**Approach**	**Materials**	**Specific capacitance**
Li sun et al. 2013	$ZnCl_2$ activation at 900 ^oC	Waste coconut shell in KOH	210 F/g at 1 A/g
Bello et al. 2016	KOH activation at 800 ^oC	Pine cone in Na_2SO_4	137 F/g at 0.5 A/g
Feng et al. 2016	Oxygen doped KOH activation at 800 ^oC	Waste dragon fruit skin in KOH	286.9 F/g at 0.5 A/g
He et al. 2016	Microwave assisted $ZnCl_2$ activation	Rice husk in IL	157 F/g at 0.5 A/g
Wang et al. 2015	KOH activation at 850 ^oC	Corn cob in KOH	328.4 F/g at 0.5 A/g
This work	KOH activation at 800 ^oC	Waste coconut shell in KOH	300 F/g at 1 A/g
		Pine cone in KOH	205.71 F/g at 1 A/g
		Rice husk in KOH	161.17 F/g at 1 A/g

4.7 SUMMARY

It is safe to conclude that the plant waste biomass activated carbons that were synthesized are a low-cost high performance go to option for electrode materials of supercapacitor application with their characteristic low resistance values and significant specific capacitance values. The investigated biomass materials have clearly emphasized that the hydrothermal treatment

processing step is a vital step of the synthesis of activated carbon that does not present any detrimental effects to the final overall performance of the AC material as supercapacitor electrodes. Micrographs of these materials as well as the gas adsorption analysis measurement results showed good porosity and surface area properties of the chosen waste plant biomass materials. Thus, the materials under investigation show potential in applications for supercapacitor electrode materials.

With the competent electrochemical performance results obtained by calculating specific capacitance from the cyclic voltamograms and the constant current galvanostatic charge discharge curves, and generating a maximum specific capacitance of 300 F/g at 1 A/g as observed in the coconut shell sample carbonized for 3hrs requires more attention to be given to these devices to enable them get to their peak performance. Although the coconut shell is presented as the best material as per capacitance it also had some lapses with its resistance and electrochemical behavior.

CHAPTER FIVE

CONCLUDING REMARKS

5.1 CONCLUSION

In summary, a great study on electrochemical capacitors (ECs) as energy storage devices has been carried out for this work and plant waste biomass materials were sourced and successfully synthesized into ACs to serve as electrode materials of ECs. The synthesized low-cost porous carbons were also investigated through various measurement and characterization techniques. Some selected results have also been presented alongside the significance of such results. A maximum specific capacitance of 300 F/g at 1 A/g was obtained showing potential of the biomass sourced activated carbon in energy storage and power delivery applications.

5.2 FUTURE WORK

There is need for more work to be done by clearly understanding and improving the individual intrinsic properties of the materials in supercapacitor electrodes since it is one of the vital and key parameters to optimizing the energy storage density of a device. Focus should also be placed on understanding the thermal stability of the system through measurements such as the thermo gravimetric analysis furthermore. It is also crucial for the electrodes to undergo investigation in the two-coin electrode configuration since the standard and true electrochemical performance of the materials is usually detected in the two-cell setup. Also, further research should be carried out on incorporating other materials to improve performance as in the case of an asymmetric performance for a good boost of the storage density of the electrochemical capacitors.

REFERENCES

Chapter One

1. Cheng Zhong et al. A review of electrolyte materials and compositions for electrochemical supercapacitors Chem. Soc. Rev., 2015, 44, 7484

Chapter Two

1. F. Barzegar et al. Asymmetric supercapacitor based on an a-MoO3 cathode and porous activated carbon anode materials; RSC Adv., 2015, 5, 37462
2. Meryl D. Stoller and Rodney S. Ruoff. Best practice methods for determining an electrode material's performance for ultracapacitors; RSC Energy Environ. Sci., 2010, 3, 1294–1301
3. Aiping Yu et al. Electrochemical supercapacitors for energy storage and delivery: Fundamentals and applications; 2013 CRC Press, Taylor and Francis Group Boca Raton
4. Feynman et al. The Feynman lectures on physics vol 1-3 1963
5. Chris Woodford. Supercapacitors; explainthatstuff.com august 2015
6. Gouping Wang et al. A review of electrode materials for electrochemical supercapacitors; Chem Soc Rev 2012, 41, 797–828.
7. B E Conway. Electrochemical supercapacitors: scientific fundamentals and technological applications, New York: The Kluwer Academic/Plenum, 1999
8. Cheng Zhong et al. A review of electrolyte materials and compositions for electrochemical supercapacitors; Chem. Soc. Rev., 2015, 44, 7484
9. M S Halper, J C Ellenbogen. Supercapacitors: A brief overview; MITRE Nanosystem group 2006
10. Faxing Wang et al. Electrode materials for aqueous asymmetric supercapacitors; RSC Advances, 2013, 3,13059
11. Grzegorz Lota et al. Carbon nanotubes and their composites in electrochemical applications; Energy Environ. Sci., 2011, 4, 1592–1605

12. K Jurewicz et al. Supercapacitors from nanotubes/polypyrrole composites; Chemical Physics Letters 347 (2001) 36-40
13. E. Frackowiak et al. Supercapacitors based on conducting polymers/nanotubes composites; Journal of Power Sources 153 (2006) 413–418
14. Jun Yan et al. Recent advances in design and fabrication of electrochemical supercapacitors with high energy densities; Adv. Energy Mater. 2014, 4, 1300816
15. J.A. Macia'-Agullo' et al. Activation of coal tar pitch carbon fibres: Physical activation vs. chemical activation; Carbon 42 (2004) 1367–1370
16. B. Viswanathan et al. Method of activation and specific applications of carbon materials; National centre of catalysis research, Indian Institute of Technology Madras Chennai, February 2009
17. Li Sun et al. From coconut shell to porous graphene-like nanosheets for high-power supercapacitors; J. Mater. Chem. A, 2013, 1,6462
18. Saswata Bose et al. Carbon-based nanostructured materials and their composites as supercapacitor electrodes; J. Mater. Chem., 2012, 22, 767–784
19. D Y Momodu. Investigation of metal hydroxide-graphene composites as electrode materials for supercapacitor applications; Doctoral thesis University of Pretoria, June 2015
20. Leo Daniel. Composite materials AUST lecture notes 2016
21. L Zhang et al. Graphene-based materials as supercapacitor electrodes; J. Mater. Chem., 2010, 20, 5983–5992
22. Abdulhakeem Bello et al. Renewable pine cone biomass derived carbon materials for supercapacitor application; RSC Adv., 2016, 6, 1800
23. Wanru Feng et al. Oxygen-doped activated carbons derived from three kinds of biomass: preparation, characterization and performance as electrode materials for supercapacitors; RSC Adv., 2016, 6, 5949

24. Xiaojun He et al. Synthesis of Mesoporous Carbons from Rice Husk for Supercapacitors with High Energy Density in Ionic Liquid Electrolytes; J. Nanosci. Nanotechnol. 2016, Vol. 16, No. 3
25. D. Wang et al. High performance electrode materials for electric double-layer capacitors based on biomass-derived activated carbons; Electrochimica Acta 173 (2015) 377–384

Chapter Four

1. M N Mohd Iqbaldin et al. properties of coconut shell activated carbon; Journal of Tropical Forest Science 25(4) 497-503, 2013
2. S Dinesh. Development and characterization of pellet activated carbon from new precursors; Bachelor of technology thesis, National Institute of Technology Rourkela, 2011
3. B E Conway. Electrochemical supercapacitors: scientific fundamentals and technological applications, New York: The Kluwer Academic/Plenum, 1999
4. Aiping Yu et al. Electrochemical supercapacitors for energy storage and delivery: Fundamentals and applications; 2013 CRC Press, Taylor and Francis Group Boca Raton